Short Kevlar Fiber–Thermoplastic Polyurethane Composite

SUNIL K. N. KUTTY and GOLOK B. NANDO*

Rubber Technology Centre, Indian Institute of Technology, Kharagpur, India 721 302

SYNOPSIS

Mechanical and dynamic mechanical behavior of short Kevlar fiber-filled thermoplastic polyurethane (TPU) have been studied with respect to fiber loading and orientation. The strength of the composite is improved at higher fiber content with a minimum at 10 phr of fibers. Storage and loss moduli (E', E'') are increased and tan δ_{max} is reduced progressively with fiber loading, the effect on moduli being more pronounced at post-T_g temperatures. Anisotropy in strength is evident beyond 15 phr fiber loading. Impact strength is reduced considerably at all fiber loadings irrespective of fiber orientation. Study of the fracture surface by scanning electron microscopy (SEM) shows good correlation between the modes of failure and strength of the composites. SEM study of the extracted fibers shows the existence of a kinking stage through which the fiber undergoes severe breakage during processing.

INTRODUCTION

Short-fiber composites gained importance due to the advantages in processing, mechanical properties, and low cost. Earlier works were confined to natural fibers like cellulose[1-5] and jute[6,7] in natural and synthetic elastomer matrices. It has been concluded that the mechanical properties of short-fiber rubber composites depend on fiber orientation, L/D ratio, dispersion, and fiber matrix bond strength, in addition to the respective strengths of matrix and fiber.[8-11] A tricomponent dry bonding system for improving fiber–matrix bonding has been successfully tried in many short fiber–elastomer composites.[12-14] Later, many synthetic short fibers like nylon and poly(ethylene terephthalate) also have been used as reinforcing fillers.[15-17] Aramid fiber is well known for its high strength-to-weight ratio. Even though some attempts have been made to use aramid short fibers as a reinforcing agent in the elastomer matrix,[18] its use is found to be scarce in thermoplastic elastomers. Stress relaxation[19] and rheological properties[20] of the thermoplastic polyurethane TPU–Kevlar composite has been reported. In this paper, we report the results of our studies on short Kevlar fiber-reinforced TPU. The study covers (i) the effect of fiber content and orientation on mechanical and dynamic mechanical properties and (ii) the effect of different modes of cooling and recycling on the mechanical properties. The failure surfaces have been studied using scanning electron microscopy (SEM), and an attempt has been made to correlate it with the failure modes.

EXPERIMENTAL

Formulation of the mixes are given in Table I. Kevlar staple fibers and TPU were dried at 105°C for 2 h, and the mixing was carried out in a Brabender plasticorder PLE 330, fitted with a cam-type mixing head, at a temperature of 180°C and a rotor speed of 60 rpm. The torque and temperature were recorded as a function of time. The mixing sequence is shown in Table II. The mixed stock was removed immediately and was sheeted out on a mixing mill (152 × 330 mm) by passing once at tight nip. Test samples were molded on an electrically heated hydraulic press by heating for 3 min under pressure and chilling suddenly in water. Tensile and tear

* To whom correspondence should be addressed.

Journal of Applied Polymer Science, Vol. 43, 1913–1923 (1991)
 CCC 0021-8995/91/101913-11$04.00

Table I Formulation of the Mixes

	Mix No.							
Ingredient	A	B	C	D	E	F	G	H
TPU	100	100	100	100	100	100	100	100
Kevlar	—	5	10	15	20	30	40	50

testing were done as per ASTM D412-80 and D 624-73 using Instron UTM (11 95). An impact test was carried out on a Ceast impact tester model 6545/000 as per DIN 53448. Dynamic mechanical analysis was done on a Rheovibron DDV III-EP at 11 hertz and 0.1% DSA at a linear heating rate of 3°C/min.

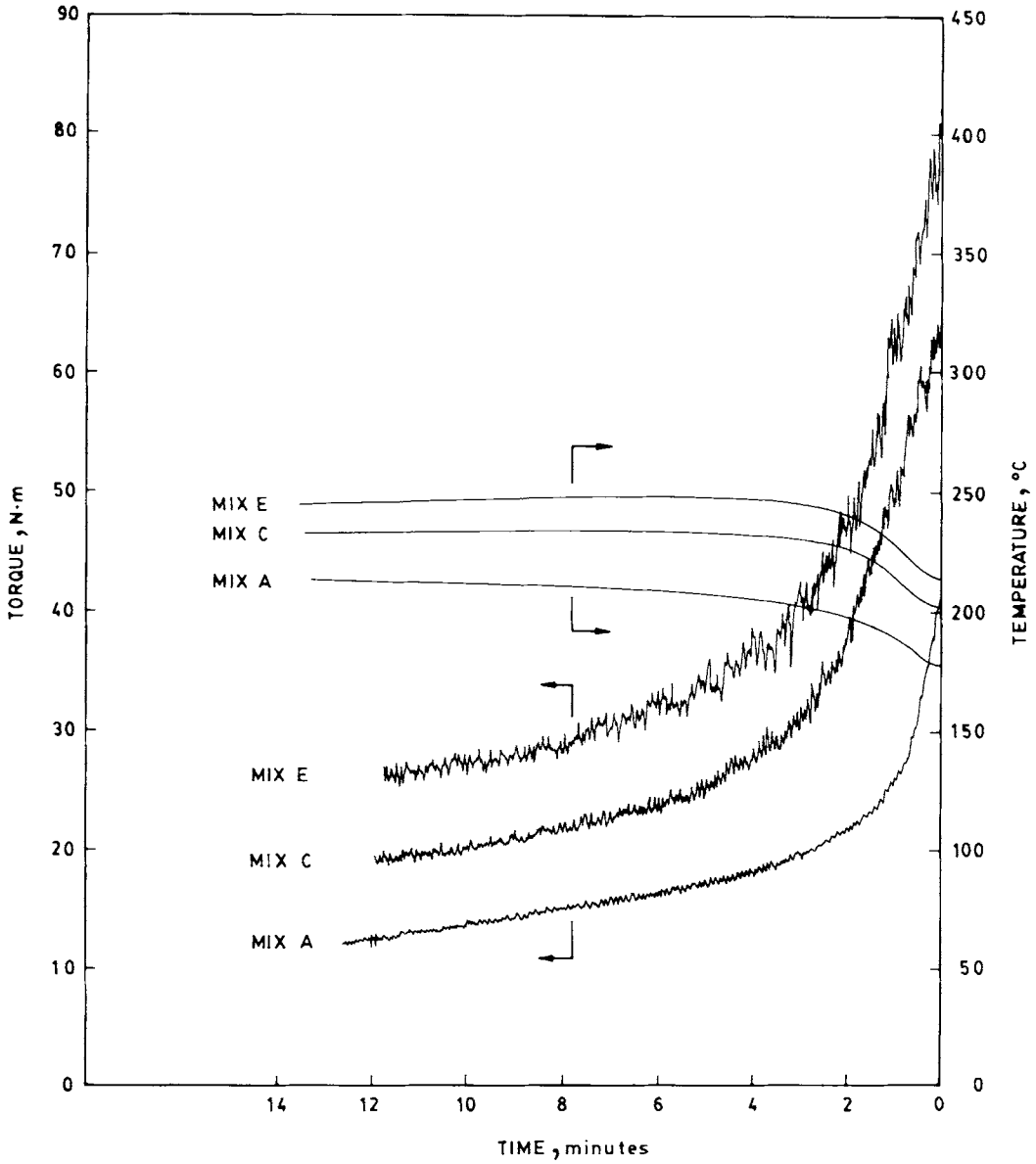

Figure 1 Brabender torque vs. time.

Table II Mixing Sequence

Ingredient	Time (min)	rpm	Ram
1/2 TPU	0	30	Up
Fiber	1.5	30	Up
1/2 TPU	3.0	60	Down
	9.0	—	Dump

RESULTS AND DISCUSSION

Processing Characteristics

Figure 1 shows the plot of Brabender torque versus time of mixing. It shows high initial torque that falls off sharply in 2–3 min and then stabilizes. This indicates a fairly good degree of dispersion within 6 min of mixing. Mixing up to 4 min and remixing for 2 more minutes after sheeting out in a two-roll mill has been reported to be more effective in obtaining good dispersion.[21] In the case of the Kevlar–TPU composite, this procedure is found to give practical difficulties in sheeting out after mixing. Therefore, for all the mixes, the mixing was done continuously for 6 min.

Fiber Breakage

Average initial fiber length was approximately 6 mm. To find the distribution of fiber length after mixing, two samples (mixes C and G) were selected. The fibers were extracted by dissolving out the matrix in solvent, and the lengths were measured using a traveling microscope. The distribution of fiber length, thus determined, are shown in Figure 2(a) and (b). In both cases, 50–60% of the fibers fall in the 0.5–1.5 mm range after mixing. The high reduction of fiber length can be attributed to the high shear that they are subjected to during mixing in the Brabender. The breakage takes place through a kinking mechanism. Fibers at kinking stage are shown in Figure 3(a). On further shearing, the kinked fibers can either break at the nodes or peel along the length. Figure 3(b) shows the end of a fiber broken at the node. For comparison, the cut end of a fiber is shown in Figure 3(c). Figure 3(d) shows a fiber at the peeling stage. Figure 3(e) and (f) shows the peeled out and unmixed fibers, respectively. It is interesting to note that the peel sometimes crosses more than one node.

Effect of the Mode of Cooling

To find the effect of the mode of cooling after molding, mix A was subjected to three modes of cooling: (1) The stock was chilled by dipping the mold in water; (2) the stock was cooled by passing water through the press platen; and (3) the stock was allowed to cool in the press under pressure in a period of 3 h. The tensile values of different stocks are given in Table III. It is found that the air-cooled sample gives the lowest strength compared to the other two.

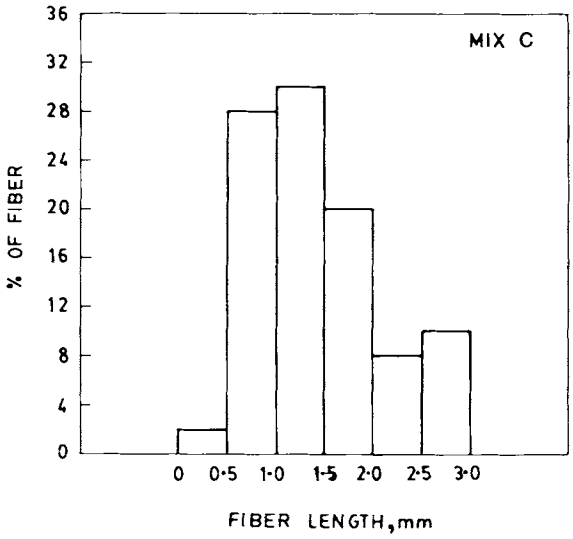

Fig. 2-a

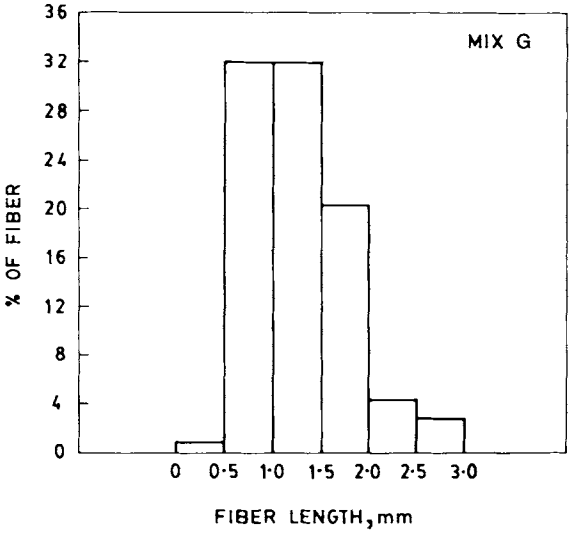

Figure 2 (a) Distribution of fiber length (mix C). (b) Distribution of fiber length (mix G).

Table III Effect of the Mode of Cooling

Mode of Cooling	Modulus at 300% (MPa)	Tensile Strength (MPa)	Elongation at Break (%)
Air cooling	8.3	30.6	690
Water cooling	8.4	36.3	630
Chilling	9.6	38.6	580

The strength values show an inverse relation to the time the stock was subjected to higher temperature and pressure. The highest strength is shown by the chilled sample, and the lowest, by the air-cooled sample. The water-cooled sample shows a value intermediate to the other two. This may be due to the higher extent of polymer degradation occurring on exposing TPU to high temperature. For TPU, molecular degradation starts above 170°C.[22]

Stress–Strain Properties

Figure 4 gives the stress–strain nature of mixes A, C, and G. A gradual change from viscoelastic to elastic response to strain is observed with fiber loading.

Table IV gives the mechanical properties of mixes A–H. The variation of tensile properties with fiber loading in the longitudinal direction is shown in Figure 5. The gum stock shows high strength and elongation at break values. This arises from the very basic structure of TPU consisting of hard and soft domains.[22] The hard segments act as virtual crosslinks and also as reinforcing filler particles. The tensile strength, which decreases sharply on incorporation of 10 phr of fibers (mix C), increases with fiber loading and then finally tends to stabilize. Similar results have been reported earlier.[23–27] The observed strength in the presence of fibers is the resultant of two opposing factors: dilution of the matrix and the reinforcement of the matrix by the fibers. At low fiber content, where the matrix is not restrained by enough fibers and high localized strains occur in the matrix at low strains, causing the bond between fiber and rubber to break and leaving the matrix diluted by nonreinforcing, debonded fibers, the dilution effect is more pronounced, whereas at

Table IV Mechanical Properties of Mixes A–H

Mix	Orientation	Tensile Strength (MPa)	Modulus at 20% (MPa)	Elongation at Break (%)	Impact Strength ($\times 10^{-3}$ J/m)	Harndess Shore A
A	L	36.5	1.2	580	—	81
	T	36.7	1.7	630	—	—
B	L	30.0	7.0	400	—	83
	T	30.0	6.5	420	—	—
				90		
C	L	16.7	11.6	nt1.09	88	
	T	13.8	5.8	540	2.15	—
D	L	24.0	16.6	48	—	88
	T	13.0	6.2	15	—	—
E	L	26.0	23.0	39	1.15	90
	T	15.5	8.3	120	1.48	—
F	L	37.9	34.0	27	1.16	92
	T	19.6	11.0	57	1.38	—
G	L	44.0	44.0	20	1.43	93
	T	21.4	14.3	55	1.36	—
H	L	58.4	54.5	22	—	93
	T	26.6	21.7	32	—	—

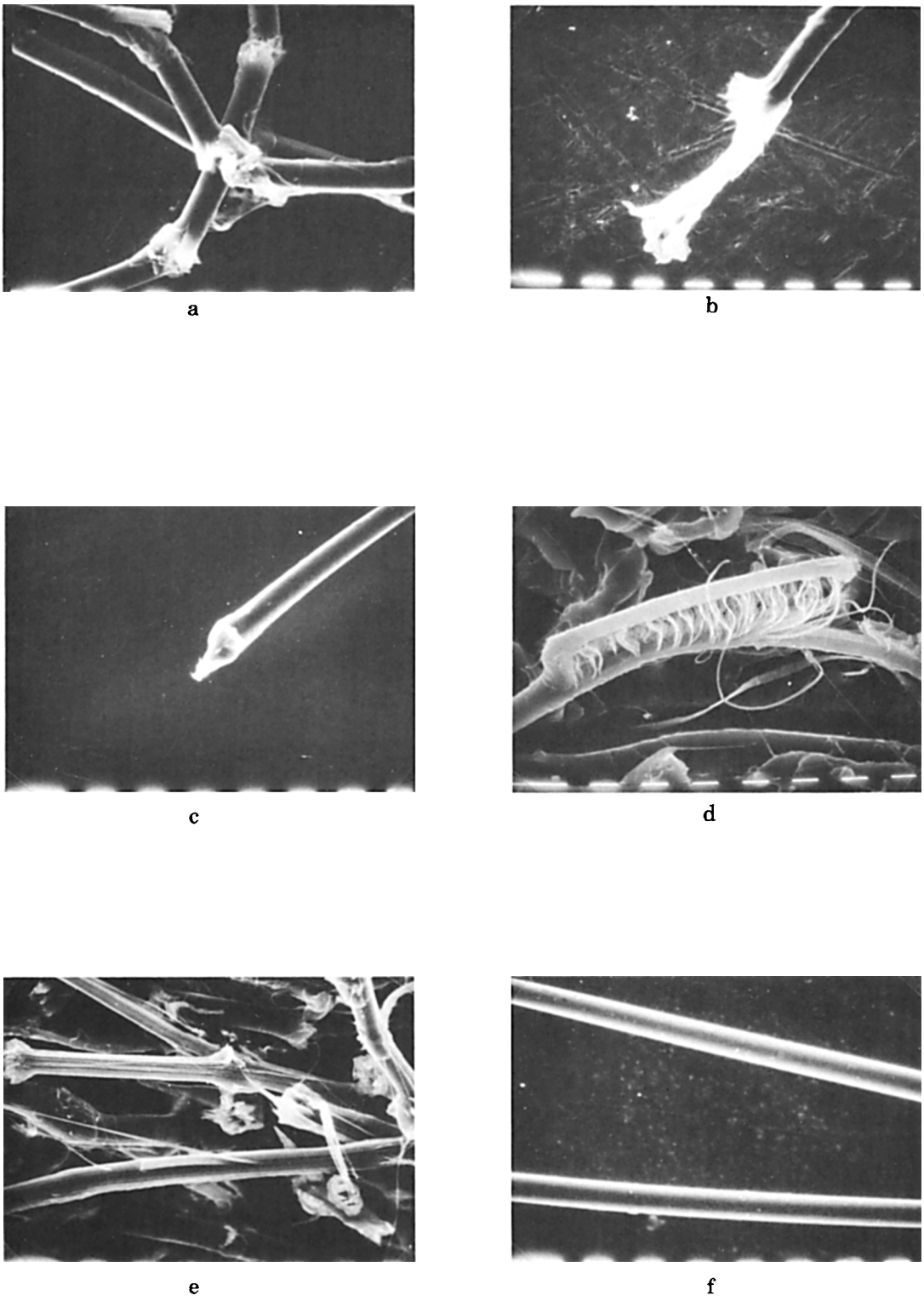

Figure 3 (a) Kevlar fiber at the kinking stage (marker = 10 μ). (b) Broken end of Kevlar fiber (marker = 10 μ). (c) Cut end of Kevlar fiber (marker = 10 μ). (d) Kevlar fiber at the peeling stage (marker = 10 μ). (e) Peeled-out Kevlar fiber (marker = 10 μ). (f) Unmixed fiber surface (marker = 10 μ).

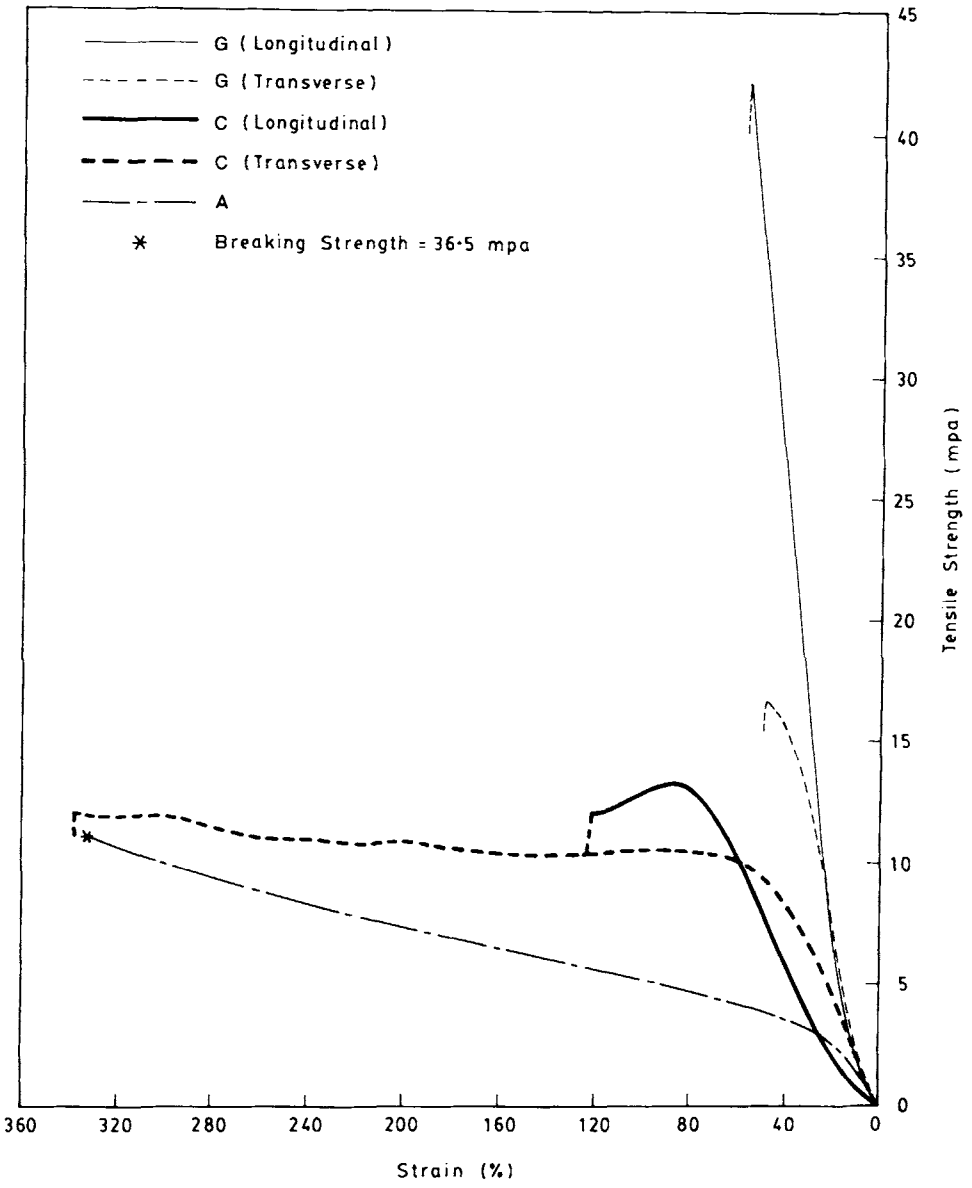

Figure 4 Stress–strain behavior of Kevlar–TPU composite.

higher fiber loading, where the matrix is sufficiently restrained and the stress is more evenly distributed, the reinforcement effect outweighs the dilution effect.[26,27] The reinforcement effect of Kevlar fibers in the TPU matrix is also evident from the dynamic mechanical studies, as explained below. SEM study of the failure surface also supports this view. SEM fractograph of the tensile fracture surface of mix C in the longitudinal direction is shown in Figure 6(a). The fiber pullouts taking place are manifested on the surface as deep holes. Some of the pulled-out fibers oriented in the direction of propagation of fracture is also seen in the figure. This is in agreement with the low strength exhibited by mix C. Tensile fractograph of mix F [Fig. 6(b)] shows fibers oriented longitudinally and "V"-shaped preferential orientation of fibers due to the propagation of tear. On magnification [Fig. 6(c)], it shows the broken fiber ends, indicating that the failure takes place mainly by fiber breakage. This is in agreement with the higher strength exhibited by mix F.

The modulus at 20% elongation shows a linear relation with fiber content. This indicates that at very low deformations when the fibers are not pulled

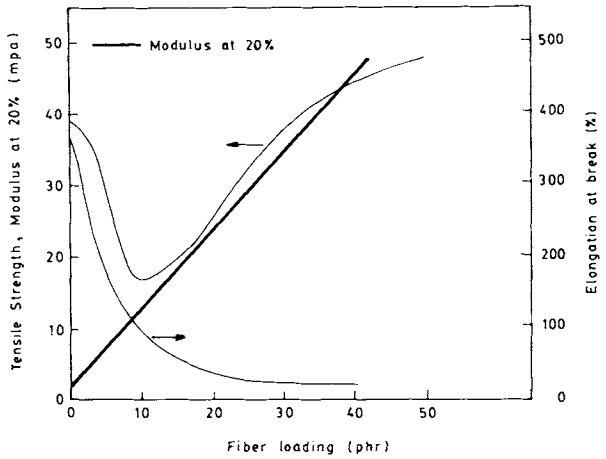

Figure 5 Variation of tensile strength with fiber content in the longitudinal direction.

out the matrix is restrained at all fiber loadings. The ultimate elongation of the gum stock finds a sharp fall at 10 phr fiber loading, beyond which the ultimate elongation remains more or less independent of fiber loading.

Variation of tensile properties with fiber loading in the transverse direction is shown in Figure 7. The tensile strength, elongation at break, and modulus with fiber loading follow the same pattern as in the longitudinal direction. However, the strength in the transverse direction is lower than that in the longitudinal direction at all fiber loading. This is because in the longitudinal direction where the fibers are oriented perpendicular to the tear path the fibers carry part of the load being transmitted through the matrix and they also serve to deflect or arrest the propagation of the fracture path that results in

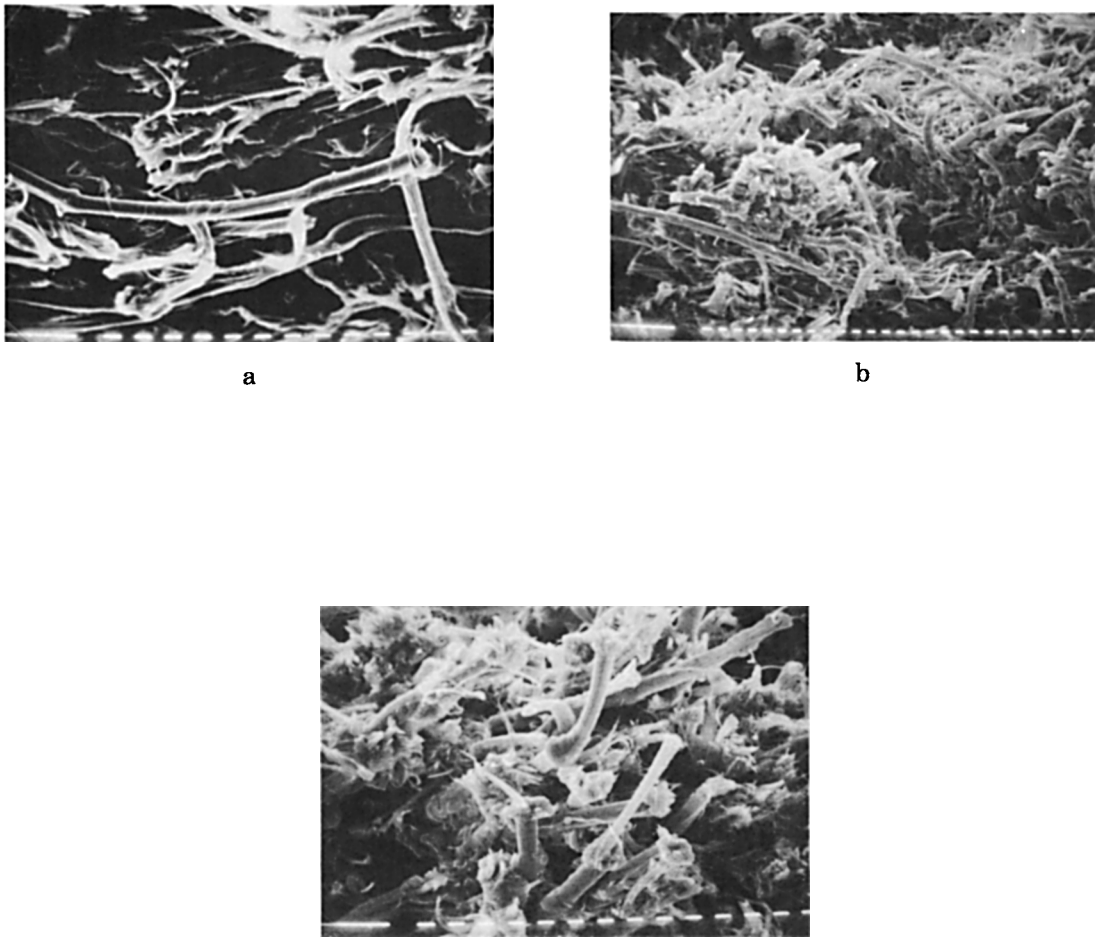

a b c

Figure 6 (a) Tensile fractograph of mix C (longitudinal direction); marker = 10 μ. (b) Tensile fractograph of mix F (longitudinal direction); marker = 10 μ. (c) Magnified view of the tensile fractograph of mix F (b); marker = 10 μ.

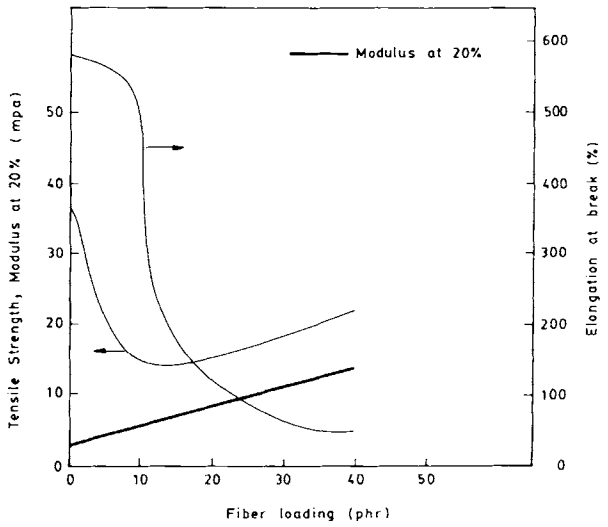

Figure 7 Variation of tensile strength with fiber loading in the transverse direction.

higher strength. In the transverse direction, the fibers, being parallel to the tear path, fail to arrest the fracture front; rather, the tear can propagate easily through the fiber–matrix interface, resulting in lower strength. SEM study of the tensile fracture surface also supports this view. Figure 8(a) shows the tensile fracture surface of mix C in the transverse direction. Holes seen on the surface are indicative of interfacial failure. Tensile fracture surface of mix F [Fig. 8(b)] shows the exposed fibers oriented in the transverse direction, which also suggests an interfacial failure.

Effect of Recycling

Recycling has a detrimental effect on the Kevlar-TPU composite, as is evident from Table V. Tensile strength is reduced drastically when molded from a remixed stock. This may be due to a high level of polymer chain breakdown during prolonged exposure to high shear and temperature.

Impact Strength

Impact strengths of Kevlar–TPU composites are shown in Table IV. Impact strength is reduced drastically in the presence of 10 phr of fibers in both directions and remains more or less constant with further increments in fiber loading. In the transverse direction, the impact strength is found to be slightly higher at lower fiber loading. However, at 40 phr loading, the anisotropy in impact strength is not apparent. The reduction of impact strength in the presence of fibers is also indicated by the smaller area under the curve in the stress–strain relationship of the filled stocks. SEM fractograph of mix C [Fig. 9(a)] shows a layer delamination type of failure of the matrix and the fiber-pulled-out holes. In the transverse direction also [Fig. 9(b)], the holes due to fiber pullout are seen. The preferential orientation of fibers in the transverse direction can be noted. Tear is found to propagate through the fiber–matrix interface.

Dynamic Mechanical Analysis

Figure 10 shows the storage modulus (E') of the mixes A–G. The storage modulus is found to increase progressively with fiber loading, the effect being more pronounced in the post-glass transition temperatures ($>T_g$). This is in agreement with the observed trend in the tensile modulus with respect to fiber loading. The increase in modulus in the presence of filler can be attributed to the reinforcement

Table V Effect of Recycling

		After One-Time Mixing			After Two Times Mixing		
Mix	Orientation	Tensile Strength (MPa)	Elongation at Break (%)	Tear Strength (kN/m)	Tensile Strength (MPa)	Elongation at Break (%)	Tear Strength (kN/m)
B	L	30	400	108	12.6	460	109
	T	30	400	109	21.3	694	108
D	L	24	47	100	17.5	82	107
	T	13	14	114	14.3	810	110

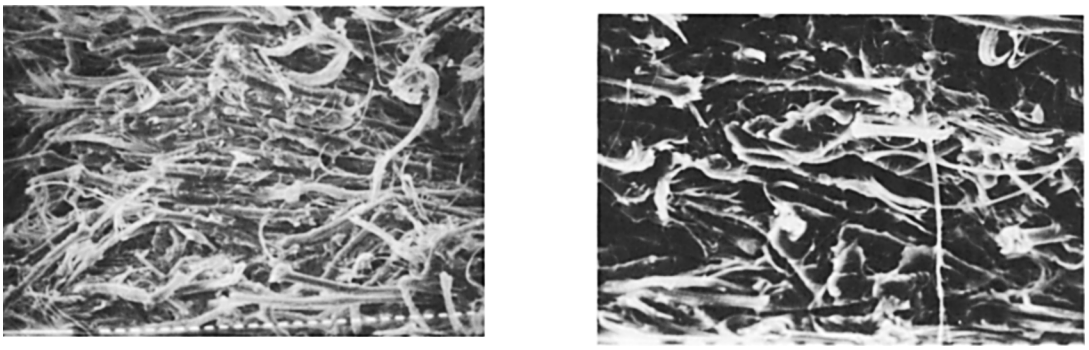

a b

Figure 8 (a) Tensile fractograph of mix C (transverse direction); marker = 10 μ. (b) Tensile fractograph of mix F (transverse direction); marker = 10 μ.

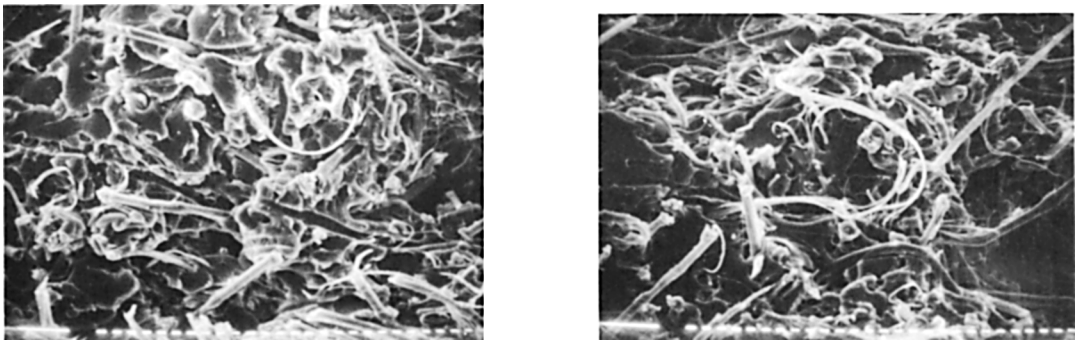

a b

Figure 9 (a) SEM photomicrograph of the impact failure surface of mix C in the longitudinal direction; marker = 10 μ. (b) SEM photomicrograph of the impact failure surface of mix C in the transverse direction; marker = 10 μ.

of the matrix by the fillers.[28] However, the glass transition temperature remains unaltered at all fiber loadings studied (Table VI).

The plateau region ($>T_g$) is found to extend over a wider range of temperature progressively with fiber loading. The larger plateau region implies continuance of the predominantly elastic nature over a wider range of temperature.

Loss tangent (tan δ) of the mixes A–G in the longitudinal direction are shown in Figure 11. It can be seen that even though T_g remains more or less constant the transition peak progressively broadens. The broadening of the tan δ peak in the presence of fillers can be ascribed to polymer–filler interaction. The polymer in the immediate vicinity of a filler particle can be thought to be in a different state as compared to the bulk matrix. This can affect the relaxation of the matrix, resulting in a broad loss tangent peak.[29] This view is again supported by the work carried out by Dutta and Tripathy[30] in which they have reported that the tan δ peak of bromobutyl vulcanizate does not undergo any appreciable change

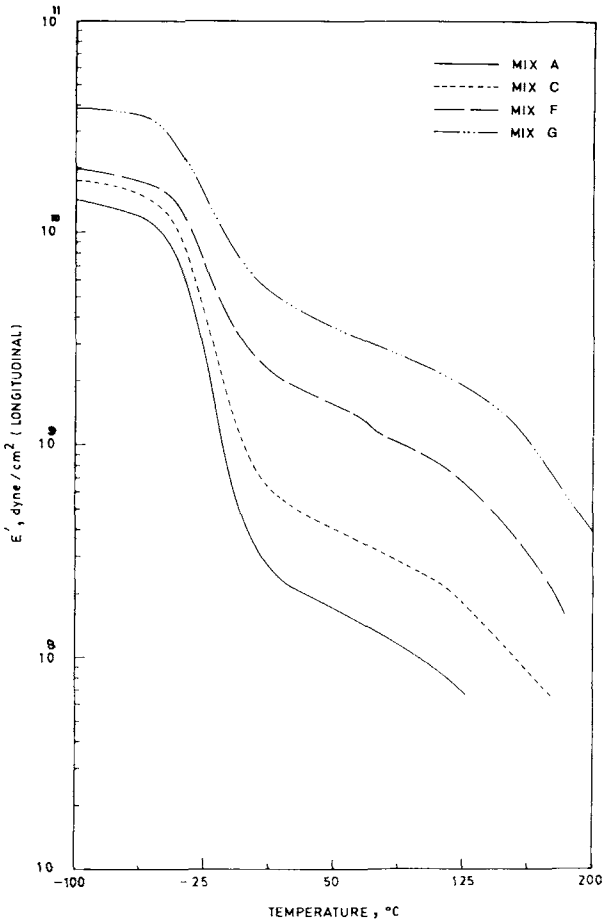

Figure 10 Storage modulus (E') vs. temperature.

in shape in the presence of glass beads because of noninteraction of the glass beads with the elastomer matrix.

The tan δ_{max} is found to decrease with fiber content, indicating a better damping characteristic of the Kevlar–TPU composite. These observations are in agreement with the results reported earlier in the case of filled elastomer vulcanizates.[28,31-33]

Table VI T_g and Tan δ_{max} from DMA

	T_g From		
Mix	E'	Tan δ	Tan δ_{max}
A	−22.1	−15.5	0.42
C	−20.2	−15.5	0.32
F	−20.2	−16.5	0.22
G	−20.2	−16.5	0.19

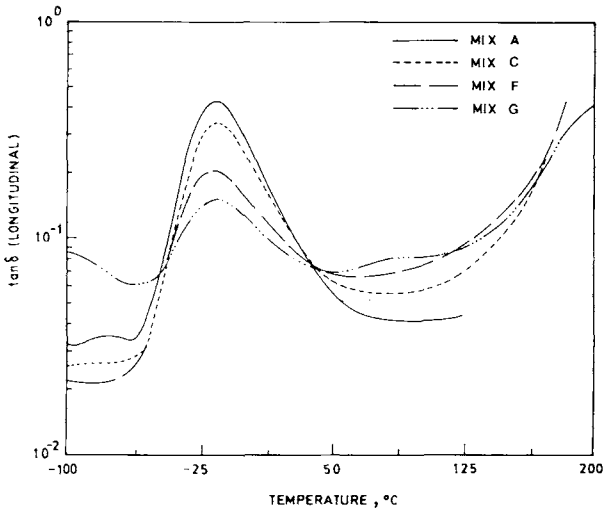

Figure 11 Loss tangent (tan δ) vs. temperature.

REFERENCES

1. P. M. Goodloe, D. H. McMurtie, and R. J. Von Nostrand, *Rubber Age,* **67,** 687 (1950).
2. P. M. Goodloe, T. L. Reiling, and D. H. McMurtie, *Rubber Age,* **61,** 697 (1947).
3. K. Boustany and A. Y. Coran, U. S. Pat. 3,697,364 (Oct. 10, 1972) (to Monsanto Co.).
4. L. A. Goettler and K. S. Shen, *Rubber Chem. Technol.,* **56,** 619 (1983).
5. B. K. I. Ku Abd Rahman and C. Hepburn, Paper presented at the International Rubber Conference on Structure Property Relations of Rubber, Kharagpur, India, 1980.
6. S. K. Chakraborty, D. K. Setua, and S. K. De, *Rubber Chem. Technlol.,* **55,** 1286 (1982).
7. V. M. Murty and S. K. De, *Rubber Chem. Technol.,* **55,** 287 (1982).
8. G. C. Derringer, *Rubber World,* **165,** 245 (1971).
9. J. E. O'Connor, *Rubber Chem. Technol.,* **50,** 945 (1977).
10. G. C. Derringer, *J. Elastoplast.,* **3,** 230 (1971).
11. K. Boustany and R. L. Arnold, *J. Elastoplast.,* **8,** 160 (1976).
12. J. R. Creasey and M. P. Wagner, *Rubber Age,* **100**(10), 72 (1968).
13. N. L. Hewitt, *Rubber Age,* **104**(1), 59 (1972).
14. E. Morita, *Rubber Chem. Technol.,* **53,** 795 (1980).
15. A. K. Senapati, G. B. Nando, and B. Pradhan, *Int. J. Polym. Mater.,* **12,** 73 (1988).
16. A. K. Senapati, S. K. N. Kutty, B. G. B. Nando, and B. Pradhan, *Int. J. Polym. Mater.,* **12,** 203 (1989).
17. S. K. N. Kutty and G. B. Nando, *Kautschuk Gummi Kunststoffe,* **43**(3), 189 (1990).

18. L. Bergomi, *Ger. Offen.* Pat. 2,115,444 (Nov. 4, 1971) (to Pirelli S.P.A.).
19. S. K. N. Kutty and G. B. Nando, *J. Appl. Polym. Sci.*, (in press).
20. S. K. N. Kutty, P. P. De, and G. B. Nando, in *International Rubber Conference 89,* Prague, and later published in *Plastics, Rubber and Composites Processing and Applications,* **15**(1), 23 (1991).
21. S. Akhtar, P. P. De, and S. K. De, *J. Appl. Polym. Sci.,* **32**(5), 5123 (1986).
22. B. M. Walker, Ed., *Handbook of Elastomers,* Van-Nostrand Reinhold, New York, 1979.
23. D. K. Setua and S. K. De, *Rubber Chem. Technol.,* **56,** 808 (1983).
24. V. M. Murty and S. K. De, *J. Appl. Polym. Sci.,* **27,** 4611 (1982).
25. J. M. Campbell, *Prog. Rubber Technol.,* **41,** 43 (1978).
26. K. Boustany and P. Hamed, *Rubber World,* **171,** 39 (1974).
27. A. Voet and J. C. Morawski, *Rubber Chem. Technol.,* **47,** 758 (1974).
28. A. I. Medalia, *Rubber Chem. Technol.,* **51,** 437 (1978).
29. J. R. M. Radok and C. L. Tai, *J. Appl. Polym. Sci.,* **6**(23), 518 (1962).
30. N. K. Dutta and D. K. Tripathy, *Kautsch. Gummi, Kunstst.,* **42,** 665 (1989).
31. D. R. Hazelton and R. C. Puydak, *Rubber Chem. Technol.,* **44,** 1043 (1971).
32. J. D. Ulmer, V. E. Chirico, and E. C. Scott, *Rubber Chem. Technol.,* **46,** 897 (1973).
33. J. D. Ulmer, W. M. Hegs, and V. E. Chirico, *Rubber Chem. Technol.,* **47,** 729 (1974).

Received February 6, 1990
Accepted January 14, 1991